ACS OMEGA

http://pubs.acs.org/journal/acsodf

Article

Probing the Site-Specific Reactivity and Catalytic Activity of Ag_n (n = 15−20) Silver Clusters

Insha Anis, Mohd. Saleem Dar, Gulzar Ahmad Bhat,* Ghulam Mohammad Rather, and Manzoor Ahmad Dar*

Cite This: *ACS Omega* 2022, 7, 19687−19693

Read Online

ACCESS | Metrics & More | Article Recommendations | Supporting Information

ABSTRACT: Density functional theory calculations within the framework of generalized gradient approximation (GGA), meta-GGA, and local functionals were carried out to investigate the reactivity and catalytic activity of Ag_n (n = 15−20) clusters. Our results reveal that all the Ag_n clusters in this size range, except Ag_{20}, adsorb O_2 preferably in the bridged mode with enhanced binding energy as compared to the atop mode. The O_2 binding energies range from 0.77 to 0.29 in the bridged mode and from 0.36 to 0.15 eV in the atop mode of O_2 adsorption. The strong binding in the case of the bridged mode of O_2 adsorption is also reflected in the increase in O−O bond distance. Natural bond orbital charge analysis and vibrational frequency calculations reveal that enhanced charge transfer occurs to the O_2 molecule and there is significant red shift in the stretching frequency of O−O bond in the case of the bridged mode of O_2 adsorption on the clusters, thereby confirming the above results. Moreover, the simulated CO oxidation reaction pathways show that the oxidation of the CO molecule is highly facile on Ag_{16} and Ag_{18} clusters involving small kinetic barriers and higher heats toward CO_2 formation.

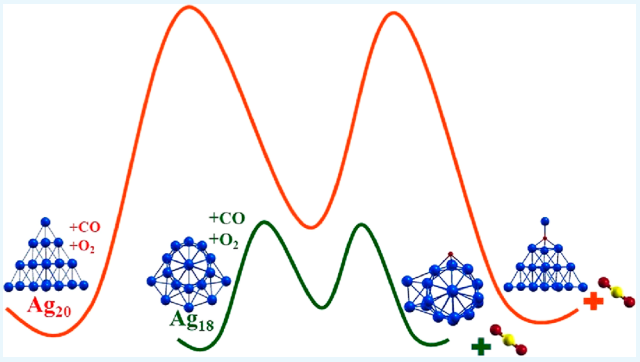

INTRODUCTION

Silver in the nano and sub-nano size regime has attracted a great deal of attention due to its wide range of catalytic and optical properties. This has led to many interesting experimental studies involving the synthesis and application of silver nanoclusters for catalyzing a wide range of reactions which include NO reduction,[1] reactions involving hydrocarbons,[2−21] and CO oxidation.[22−31] Despite the progress during the past decade to synthesize silver clusters supported on variable supports and their subsequent applications, an exact understanding of the reaction mechanism and underlying factors which govern the silver cluster reactivity is still lacking due to the complexity of heterogeneous catalysis.

Compared to the supported metal clusters, simple gas-phase clusters are considered ideal to understand the reaction mechanism and factors governing the catalytic properties of metal clusters. The stability of gas-phase clusters and the lack of direct experimental probes to understand their structure pose a great challenge in this direction. However, recent advances in experimental techniques aided by first-principles calculations have resulted in a number of studies to understand the structure and reactivity of silver nanoclusters with small molecules such as O_2. Most of these studies were carried out on small anionic Ag_n (n = 1−10) clusters as their geometric and electronic structures are easily accessible through photoelectron spectroscopy. For example, a joint experimental and theoretical study[32] revealed a pronounced size and structure dependence of O_2 binding on Ag_n^- (n = 1−5) clusters. The O_2 binding exhibited significant odd−even oscillations with the open-shell clusters showing significantly enhanced O_2 adsorption in comparison to closed-shell counterparts. Moreover, the authors found that a pre-adsorbed oxygen molecule on the closed-shell Ag_3^- and Ag_5^- significantly enhances the binding and activation of the second O_2 molecule. Socaciu et al.[33] carried out an identical type of investigation on the interaction of Ag_n^- clusters (n = 1−11) with oxygen and carbon monoxide molecules. The cluster anions were found to readily react with O_2 molecules and showed a parallel type of odd−even O_2 binding pattern. Castleman and co-workers[34] reached similar conclusions while investigating the interaction of O_2 with Ag_n^- clusters (n = 1−17) using synergistic experimental and theoretical calculations. It was found that clusters with an even number of electrons exhibit markedly less reactivity than those with an odd number of electrons toward O_2 molecules.

Received: March 10, 2022
Accepted: May 16, 2022
Published: May 27, 2022

https://doi.org/10.1021/acsomega.2c01437
ACS Omega 2022, 7, 19687−19693

Further, Ag_{13}^- was identified as a highly stable cluster due to its large highest occupied molecular orbital−lowest unoccupied molecular orbital gap and large spin excitation energy. Ma et al.[35] using kinetic measurements on reactions of Ag_n^- (n = 6−69) with O_2 revealed that reactivity of anionic silver clusters with O_2 in the nano size domain is still dominated by global electronic properties such as the spin state and electron binding strength of the cluster.

Compared to anionic silver clusters, the interaction of O_2 molecules with neutral silver clusters is less explored due to the lack of direct experimental probes. In this context, machine learning and density functional theory (DFT) act as suitable tools to probe the structure and properties of such materials.[36−48] This has mostly resulted in theoretical calculations based on DFT to evaluate the O_2 reactivity of neutral silver clusters. For example, DFT calculations by Klacar et al.[49] on the binding strength of molecular and dissociative adsorption of oxygen showed marked odd−even oscillations with the dissociative adsorption being more favorable than molecular adsorption on silver clusters with more than five atoms. Wang et al.[50] using the particle swarm and minimum hopping approach in combination with DFT calculations studied the dissociative chemisorption of O_2 on Ag_n and $Ag_{n-1}Ir$ (n = 3−26). The results pointed that O_2 dissociation entails very high barriers for clusters with n = 11−26 for both pristine and doped counterparts. DFT calculations by Liao et al.[51] also revealed odd−even oscillation in the O_2 adsorption energies on neutral silver clusters.

Although impressive progress has already been done in decoding the reactivity/catalytic behavior of small silver clusters, more effort needs to be put in to understand the catalytic activity of medium and large silver nanoclusters. Thus, in this work, we have carried out comprehensive DFT calculations on structurally well-characterized Ag_n (n = 15−20) clusters to investigate their site-dependent reactivity toward O_2 molecules. Further, followed by O_2 adsorption, we also simulated the CO oxidation reaction to understand the catalytic properties of these clusters.

COMPUTATIONAL DETAILS

All the calculations were accomplished by using DFT with Perdew−Burke−Eernzerhof (PBE), Tao−Perdew−Staroverov−Scuseria (TPSS), and M06-L functionals as implemented in the Gaussian-16[52] software. The geometry optimizations were carried out by using the Berny algorithm with the default convergence criterion. Vibrational frequency calculations were carried out to confirm the true ground-state nature of the optimized structures. To simulate the reactivity of Ag_n clusters, O_2 adsorption was studied at different possible sites in the atop mode with one Ag−O bond and the bridged mode with two to three Ag−O bonds. Furthermore, O_2 adsorption was investigated for both the singlet and triplet multiplicities for even electron clusters and doublet and quartet multiplicities for odd electron clusters. O_2 preferentially adsorbs in doublet multiplicity on the odd electron clusters and triplet multiplicity on even electron clusters expect for Ag_{16} where singlet multiplicity is the favored spin state. The LANL2DZ basis set and the corresponding Los Alamos relativistic effective core potential were used for the silver atoms, and the TZVP basis set was used for carbon and oxygen atoms. TZVP types of basis sets have been widely used for interactions of small molecules with transition metals and clusters.[53−56]

The binding energy (E_b) of the O_2 molecule was computed using the below formula

$$E_b = E_{O_2} + E_{Ag_n} - E_{Ag_nO_2}$$

where E_{O_2} is the energy of the O_2 molecule in the triplet state, E_{Ag_n} is the energy of the isolated cluster, and $E_{Ag_nO_2}$ is the energy of the O_2-adsorbed Ag_n complex. The transition states for simulating CO oxidation pathways on Ag_n clusters were found by using the linear synchronous transit method and were characterized by the presence of one imaginary frequency.

RESULTS AND DISCUSSION

We proceed with a discussion on the adsorption of the O_2 molecule on the different sites of Ag_n (n = 15−20) clusters. The lowest-energy structures of Ag_n clusters are in the size range of n = 15−20 atoms as presented in Figure 1 and are

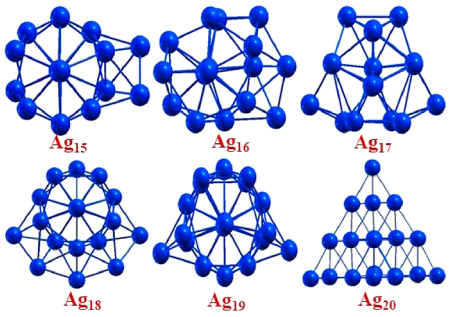

Figure 1. Ground-state structures of Ag_n (n = 15−20) clusters obtained using the PBE functional.

already well documented by previous studies.[34] To characterize O_2 reactivity of these clusters, we first adsorbed O_2 in atop and bridged modes at the different possible sites in these clusters as shown in Figures S1 and S2. The optimized geometries of the lowest-energy Ag_nO_2 complexes in both the bridged and atop modes with their relative energies in eV are displayed in the Figure 2. As can be seen, O_2 preferentially undergoes the bridged type of bonding with all the silver clusters except Ag_{20}, which shows the atop mode of bonding with O_2. The energy difference between the bridged and atop modes is particularly pronounced for $Ag_{16}O_2$ and $Ag_{17}O_2$ clusters. In the case of $Ag_{20}O_2$, the atop mode of adsorption is stronger with no bridged adsorption involving both oxygen atoms bonded to Ag atoms. It is noteworthy to mention here that earlier reports by Liao et al.[51] contrastingly pointed the atop mode of O_2 binding as the most favorable adsorption on Ag_{15}−Ag_{18} clusters. To further confirm our results, we optimized the structures using TPSS and M06-L functionals. The results also revealed the bridged O_2 binding on all Ag_n clusters except Ag_{20} rather than atop mode of binding.

The interaction of molecular oxygen can be quantitatively understood in terms of the O_2 binding energies on the Ag_n clusters. Tables 1 and 2 enlist the computed O_2 binding energies in bridged and atop modes, respectively, obtained by PBE, TPSS, and M06-L functionals with excellent agreement for all the clusters under consideration. As can be seen, all the silver clusters except Ag_{20} show higher binding energies in the bridged mode as compared to the atop mode. Further, the O_2 binding energies decrease as we go from Ag_{15} to Ag_{19} in the bridged mode with Ag_{18} showing the lowest binding energy of 0.29 eV and Ag_{15} and Ag_{16} showing the highest binding

https://doi.org/10.1021/acsomega.2c01437
ACS Omega 2022, 7, 19687−19693

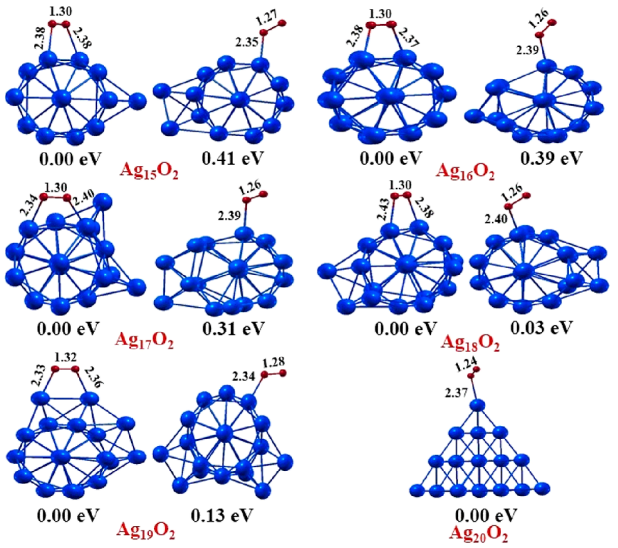

Figure 2. Lowest-energy bridged and atop configurations of O_2 adsorption on Ag_n clusters (n = 15−20), with their relative energies and relevant geometrical parameters computed at the PBE level of theory.

energies of 0.77 and 0.66 eV, respectively, at the PBE level of theory. Moreover, the odd−even trends in the bridged mode of O_2 binding energy are not quite visible in the studied cases, which is in sharp contrast to small silver clusters having less than 10 atoms. The atop mode of adsorption reveals significantly lower binding energies with strong odd−even oscillation. The enhanced binding of O_2 adsorption is reflected in the significant increase in the O−O bond distances in the bridged mode as compared to the atop mode of O_2 adsorption. The bridged Ag_n−O_2 complexes reveal an average O−O bond distance of ∼1.30 Å, whereas atop Ag_n−O_2 complexes reveal an average O−O bond distance of ∼1.26 Å. The above results are corroborated by natural bond orbital (NBO) charges on O_2. As can be seen in Tables 1 and 2, the bridged mode of adsorption leads to a significantly higher charge transfer of ∼0.40 e to O_2 as compared to ∼0.25 e in the case of atop adsorption. Further, a significant amount of red shift corresponding to the O−O frequency in the bridged mode compared to the atop mode of the O_2 adsorption also reflects the strong activation of the O−O bond.

We next looked at the CO oxidation ability of Ag_n clusters using the Langmuir−Hinshelwood mechanism. In the Langmuir−Hinshelwood type of reaction mechanism, the O_2 and CO molecules first co-adsorb on the adjacent sites of a cluster, leading to the formation of the O−O−C−O intermediate in the first step and release of the CO_2 molecule in the second step. Figure 3 displays the structures and relative energies of the involved reactants, intermediates, transition states, and final products on the Ag_n clusters. The lowest-energy configurations of O_2 and CO co-adsorbed Ag_n clusters were obtained by adsorbing CO molecules on different possible sites next to the adsorbed O_2 on the clusters. From Figure 3, we note that the first step leading to the formation of the O−O−C−O intermediate on Ag_{20} involves a very high activation barrier of 0.55 eV. The second step involving the cleavage of the O−O bond of the O−O−C−O intermediate and leading to the release of CO_2 entails a barrier of 0.22 eV. However, with the activation of molecular oxygen and O−O−C−O intermediate formation being the rate-determining step for CO oxidation on metal clusters,[57−62] CO oxidation reaction on Ag_{20} is less feasible. Contrary to this, for Ag_{15} to Ag_{19}, the first step leading to the formation of the O−O−C−O intermediate involves very low activation barriers of 0.11, 0.18, 0.15, 0.01, and 0.14 eV, respectively. The reaction barriers for the second step are 0.40, 0.31, 0.33, 0.32, and 0.51 eV, respectively. Interestingly, we note that the CO oxidation reactions on the Ag_{16} and Ag_{18} clusters involve the intermediates and transition states significantly lower in energy than the rest of the clusters. This makes the reaction more facile and thereby increases the probability of the CO oxidation on the Ag_{16} and Ag_{18} clusters. NBO charge analysis along the reaction pathway of Ag_{16}, Ag_{18}, and Ag_{20} was carried out to understand the stabilization of transition states along the CO oxidation reaction pathways on Ag_{16}, Ag_{18}, and Ag_{20}. The net NBO charges on the O_2 molecule are presented in Table 3. The calculated NBO charges analysis reveals that significant charge transfer occurs from the cluster to the O_2 molecule in TSI and TS2 in the case of Ag_{16} and Ag_{18} clusters, leading to their stabilization and subsequent reduction in barrier heights. A similar trend is seen in the frontier molecular orbital analysis of TSI and TS2 (Figure S3), wherein we note significant overlap in the case of Ag_{16} and Ag_{18} compared to Ag_{20}.

Furthermore, the calculated heat of formation for the final products in the case of Ag_{16} and Ag_{18} are −3.61 and −3.22 eV, respectively. Thus, among the above-studied silver clusters, Ag_{16} and Ag_{18} are the most promising model catalysts for CO oxidation with low activation barriers.

CONCLUSIONS

In summary, we have investigated the reactivity and catalytic properties of Ag_n (n = 15−20) clusters using first-principles simulations. The findings point that the extent of O_2 adsorption depends largely on the mode of adsorption. It is found that O_2 adsorbs strongly with enhanced binding energy in the bridged mode on all the clusters except Ag_{20} as

Table 1. Binding Energies of O_2 (E_b) and Optimized Geometrical Parameters Such as Ag−O Bond Length (r_{Ag-O}), O−O Bond Length (r_{O-O}), and O−O Stretching Frequency (ν_{O-O}) and Q_{O_2} of the Ag_nO_2 in the Bridged Mode Computed Using the PBE Level of Theory

system	E_b(PBE) (eV)	E_b(TPSS) (eV)	E_b(M06-L) (eV)	r_{Ag-O} (Å)	r_{O-O} (Å)	ν_{O-O} (cm^{-1})	Q_{O_2}
$Ag_{15}O_2$	0.77	0.82	0.86	2.38/2.38	1.30	1134	−0.42
$Ag_{16}O_2$	0.66	0.89	0.87	2.37/2.38	1.30	1118	−0.43
$Ag_{17}O_2$	0.61	0.54	0.65	2.34/2.40	1.31	1106	−0.46
$Ag_{18}O_2$	0.29	0.25	0.26	2.38/2.43	1.30	1113	−0.41
$Ag_{19}O_2$	0.56	0.59	0.56	2.33/2.36	1.32	1110	−0.54
$Ag_{20}O_2$							

https://doi.org/10.1021/acsomega.2c01437
ACS Omega 2022, 7, 19687−19693

Table 2. Binding Energies of O_2 (E_b) and Optimized Geometrical Parameters Such as Ag−O Bond Length(r_{Ag-O}), O−O Bond Length (r_{O-O}), and O−O Stretching Frequency (ν_{O-O}) and Q_{O_2} of the Ag_nO_2 in the Atop Mode Computed Using the PBE Level of Theory

system	E_b(PBE) (eV)	E_b(TPSS) (eV)	E_b(M06-L) (eV)	r_{Ag-O} (Å)	r_{O-O} (Å)	ν_{O-O} (cm^{-1})	Q_{O_2}
$Ag_{15}O_2$	0.36	0.44	0.31	2.35	1.27	1244	−0.28
$Ag_{16}O_2$	0.29	0.28	0.29	2.39	1.26	1281	−0.21
$Ag_{17}O_2$	0.30	0.24	0.27	2.39	1.26	1265	−0.22
$Ag_{18}O_2$	0.25	0.24	0.36	2.40	1.26	1285	−0.17
$Ag_{19}O_2$	0.48	0.42	0.39	2.34	1.28	1228	−0.29
$Ag_{20}O_2$	0.15	0.14	0.13	2.50	1.24	1358	−0.13

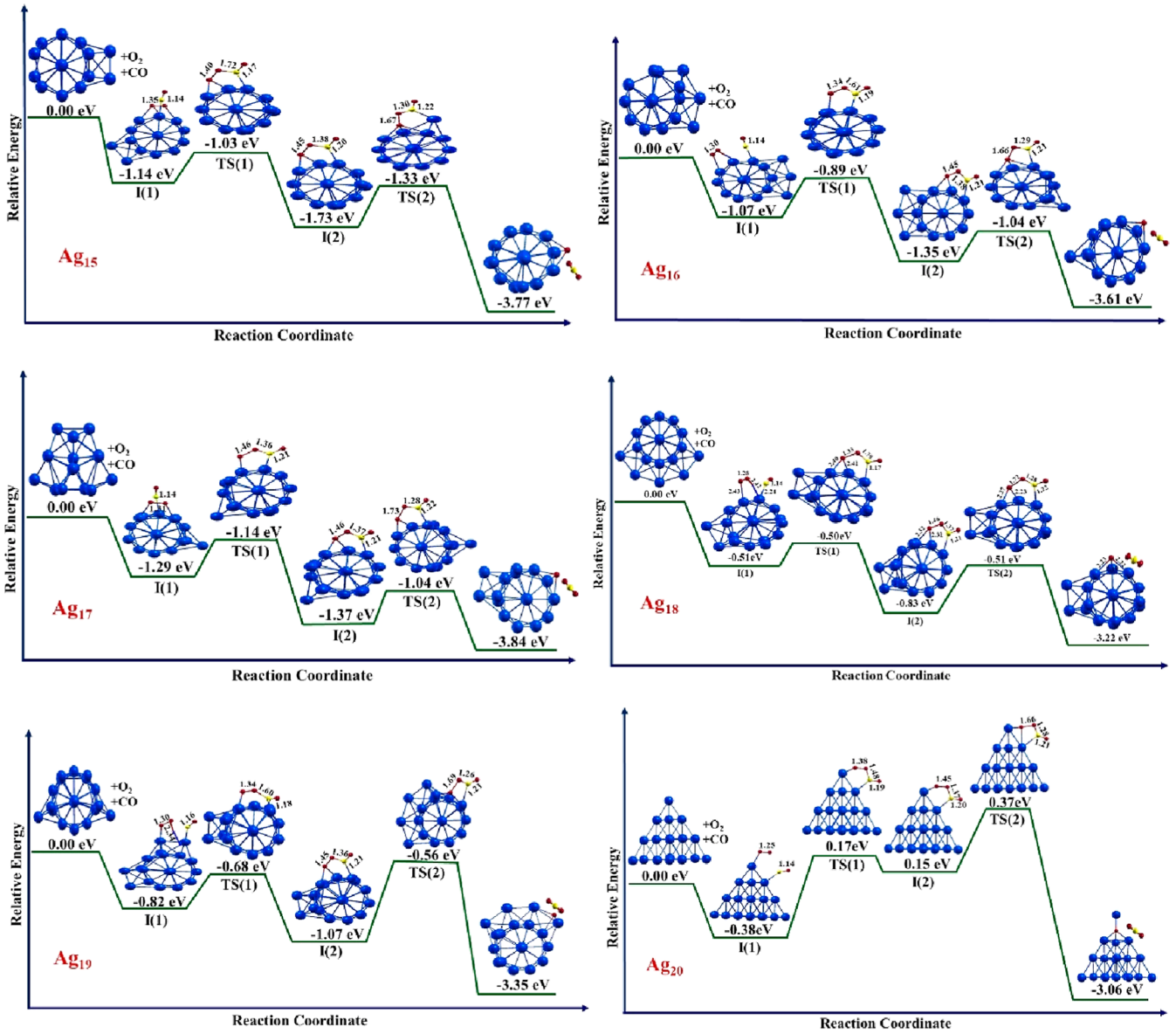

Figure 3. Simulated reaction pathways (schematic) for CO oxidation on the Ag_n clusters (n = 15−20) computed at the PBE level of theory.

Table 3. Calculated NBO Charges on O_2 along the CO Oxidation Reaction Pathway on Ag_{16}, Ag_{18}, and Ag_{20}

system	Q_{O_2} (Int-1)	Q_{O_2} (TS-1)	Q_{O_2} (Int-2)	Q_{O_2} (TS-2)
Ag_{16}	−0.40	−0.62	−0.76	−0.93
Ag_{18}	−0.25	−0.64	−0.47	−0.90
Ag_{20}	−0.18	−0.49	−0.64	−0.77

compared to the atop mode. A substantial increase in the O−O bond lengths accompanied with a pronounced red shift in the O−O frequency in the bridged adsorption also corroborates the obtained results. Simulated reaction pathways reveal that Ag_{16} and Ag_{18} clusters entail very low barriers and formation energies for CO oxidation to CO_2. Furthermore, the stabilization of transition states is reflected in the enhanced

https://doi.org/10.1021/acsomega.2c01437
ACS Omega 2022, 7, 19687−19693

NBO charge transfer to O_2 and significant spatial overlap between frontier molecular orbitals, eventually leading to their stabilization. Thus, Ag_{16} and Ag_{18} clusters act as efficient catalysts for the environmentally important CO oxidation reaction.

■ ASSOCIATED CONTENT

Supporting Information

The Supporting Information is available free of charge at https://pubs.acs.org/doi/10.1021/acsomega.2c01437.

Different configurations of O_2 adsorption and frontier molecular orbital analysis and Cartesian coordinates of optimized geometries of Ag_n, Ag_nO_2, and intermediates and transition states involved in the reaction pathway for CO oxidation on Ag_n clusters (PDF)

■ AUTHOR INFORMATION

Corresponding Authors

Gulzar Ahmad Bhat − *Center for Interdisciplinary Research and Innovations, University of Kashmir, Srinagar 190006, India*; Email: gulzarbhat@uok.edu.in

Manzoor Ahmad Dar − *Department of Chemistry, Islamic University of Science and Technology, Awantipora, Jammu and Kashmir 192122, India*; orcid.org/0000-0002-2529-5453; Email: manzoor.dar@islamicuniversity.edu.in

Authors

Insha Anis − *Department of Chemistry, Islamic University of Science and Technology, Awantipora, Jammu and Kashmir 192122, India*

Mohd. Saleem Dar − *Biochemical Sciences Division, CSIR-National Chemical Laboratory, Pune 411008, India*

Ghulam Mohammad Rather − *Department of Chemistry, Islamic University of Science and Technology, Awantipora, Jammu and Kashmir 192122, India*

Complete contact information is available at: https://pubs.acs.org/10.1021/acsomega.2c01437

Author Contributions

I.A. and M.S.D. performed the theoretical calculations. M.A.D., G.A.B., and G.M.R. conceptualized the study and carried out advising. All the authors contributed to the preparation of the manuscript.

Notes

The authors declare no competing financial interest.

■ ACKNOWLEDGMENTS

I.A. acknowledges TEQIP-III for research fellowship. M.A.D. acknowledges Start-up research grants from SERB [SRG/2020/00654] and UGC [no. F. 30-512/2020(BSR)], India, for financial support toward the completion of this work. G.A.B. gratefully acknowledges DST-SERB for the Ramanujan fellowship grant (RJF2020/000116). The authors acknowledge National Supercomputing Mission (NSM) for providing computing resources of "PARAM Brahma" at IISER Pune, which is implemented by C-DAC and supported by the Ministry of Electronics and Information Technology (MeitY) and the Department of Science and Technology (DST), Government of India.

■ REFERENCES

(1) Shimizu, K.-i.; Tsuzuki, M.; Kato, K.; Yokota, S.; Okumura, K.; Satsuma, A. Reductive Activation of O_2 with H_2-Reduced Silver Clusters as a Key Step in the H_2-Promoted Selective Catalytic Reduction of NO with C_3H_8 over Ag/Al_2O_3. *J. Phys. Chem. C* **2007**, *111*, 950−959.

(2) Shimizu, K.-i.; Miyamoto, Y.; Satsuma, A. Size-and Support-Dependent Silver Cluster Catalysis for Chemoselective Hydrogenation of Nitroaromatics. *J. Catal.* **2010**, *270*, 86−94.

(3) Claus, P.; Hofmeister, H. Electron Microscopy and Catalytic Study of Silver Catalysts: Structure Sensitivity of the Hydrogenation of Crotonaldehyde. *J. Phys. Chem. B* **1999**, *103*, 2766−2775.

(4) Grünert, W.; Brückner, A.; Hofmeister, H.; Claus, P. Structural Properties of Ag/TiO_2 Catalysts for Acrolein Hydrogenation. *J. Phys. Chem. B* **2004**, *108*, 5709−5717.

(5) Chen, Y.; Wang, C.; Liu, H.; Qiu, J.; Bao, X. Ag/SiO_2: A Novel Catalyst with High Activity and Selectivity for Hydrogenation of Chloronitrobenzenes. *Chem. Commun.* **2005**, *42*, 5298−5300.

(6) Deng, J.-P.; Shih, W.-C.; Mou, C.-Y. Electron Transfer-Induced Hydrogenation of Anthracene Catalyzed by Gold and Silver Nanoparticles. *J. Phys. Chem. C* **2007**, *111*, 9723−9728.

(7) Lim, K. H.; Mohammad, A. B.; Yudanov, I. V.; Neyman, K. M.; Bron, M.; Claus, P.; Rösch, N. Mechanism of Selective Hydrogenation of α, β-Unsaturated Aldehydes on Silver Catalysts: A Density Functional Study. *J. Phys. Chem. C* **2009**, *113*, 13231−13240.

(8) Yang, X.; Wang, A.; Wang, X.; Zhang, T.; Han, K.; Li, J. Combined Experimental and Theoretical Investigation on the Selectivities of Ag, Au, and Pt Catalysts for Hydrogenation of Crotonaldehyde. *J. Phys. Chem. C* **2009**, *113*, 20918−20926.

(9) Lei, Y.; Mehmood, F.; Lee, S.; Greeley, J.; Lee, B.; Seifert, S.; Winans, R. E.; Elam, J. W.; Meyer, R. J.; Redfern, P. C.; Teschner, D.; Schlögl, R.; Pellin, M. J.; Curtiss, L. A.; Vajda, S. Increased Silver Activity for Direct Propylene Epoxidation via Subnanometer Size Effects. *Science* **2010**, *328*, 224−228.

(10) Ghosh, S.; Acharyya, S. S.; Tiwari, R.; Sarkar, B.; Singha, R. K.; Pendem, C.; Sasaki, T.; Bal, R. Selective Oxidation of Propylene to Propylene Oxide over Silver-Supported Tungsten Oxide Nanostructure with Molecular Oxygen. *ACS Catal.* **2014**, *4*, 2169−2174.

(11) Fellah, M. F.; Onal, I. Epoxidation of Propylene on a $[Ag_{14}O_9]$ Cluster Representing Ag_2O (001) Surface: A Density Functional Theory Study. *Catal. Lett.* **2012**, *142*, 22−31.

(12) Molina, L. M.; Lee, S.; Sell, K.; Barcaro, G.; Fortunelli, A.; Lee, B.; Seifert, S.; Winans, R. E.; Elam, J. W.; Pellin, M. J. Size-Dependent Selectivity and Activity of Silver Nanoclusters in the Partial Oxidation of Propylene to Propylene Oxide and Acrolein: A Joint Experimental and Theoretical Study. *Catal. Today* **2011**, *160*, 116−130.

(13) Cheng, L.; Yin, C.; Mehmood, F.; Liu, B.; Greeley, J.; Lee, S.; Lee, B.; Seifert, S.; Winans, R. E.; Teschner, D.; Schlögl, R.; Vajda, S.; Curtiss, L. A. Reaction Mechanism for Direct Propylene Epoxidation by Alumina-Supported Silver Aggregates: The Role of the Particle/Support Interface. *ACS Catal.* **2014**, *4*, 32−39.

(14) Anumula, R.; Cui, C.; Yang, M.; Li, J.; Luo, Z. Catalytic Oxidation of Cyclohexane on Small Silver Clusters Supported by Graphene Oxide. *J. Phys. Chem. C* **2019**, *123*, 21504−21512.

(15) Sulaiman, K. O.; Sudheeshkumar, V.; Scott, R. W. J. Activation of Atomically Precise Silver Clusters on Carbon Supports for Styrene Oxidation Reactions. *RSC Adv.* **2019**, *9*, 28019−28027.

(16) Porto, V.; Buceta, D.; Domínguez, B.; Carneiro, C.; Borrajo, E.; Fraile, M.; Davila-Ferreira, N.; Arias, I. R.; Blanco, J. M.; Blanco, M. C.; Devida, J. M.; Giovanetti, L. J.; Requejo, F. G.; Hernández-Garrido, J. C.; Calvino, J. J.; López-Haro, M.; Barone, G.; James, A. M.; García-Caballero, T.; González-Castaño, D. M.; Treder, M.; Huber, W.; Vidal, A.; Murphy, M. P.; López-Quintela, M. A.; Domínguez, F. Silver Clusters of Five Atoms as Highly Selective Antitumoral Agents Through Irreversible Oxidation of Thiols. *Adv. Funct. Mater.* **2022**, 2113028.

(17) Wang, X.; Rui, Z.; Ji, H. DFT Study of Formaldehyde Oxidation on Silver Cluster by Active Oxygen and Hydroxyl Groups:

https://doi.org/10.1021/acsomega.2c01437
ACS Omega 2022, 7, 19687−19693

Mechanism Comparison and Synergistic Effect. *Catal. Today* **2020**, *347*, 124−133.
(18) Mitsudome, T.; Mikami, Y.; Funai, H.; Mizugaki, T.; Jitsukawa, K.; Kaneda, K. Oxidant-Free Alcohol Dehydrogenation Using a Reusable Hydrotalcite-supported Silver Nanoparticle Catalyst. *Angew. Chem., Int. Ed.* **2008**, *47*, 138−141.
(19) Shimizu, K.-i.; Sugino, K.; Sawabe, K.; Satsuma, A. Oxidant-free Dehydrogenation of Alcohols Heterogeneously Catalyzed by Cooperation of Silver Clusters and Acid−Base Sites on Alumina. *Chem.—Eur. J.* **2009**, *15*, 2341−2351.
(20) Shimizu, K.-i.; Sato, R.; Satsuma, A. Direct C-C Cross-Coupling of Secondary and Primary Alcohols Catalyzed by a Γ-Alumina-Supported Silver Subnanocluster. *Angew. Chem.* **2009**, *121*, 4042−4046.
(21) Wu, D.-Y.; Liu, X.-M.; Huang, Y.-F.; Ren, B.; Xu, X.; Tian, Z.-Q. Surface Catalytic Coupling Reaction of P-Mercaptoaniline Linking to Silver Nanostructures Responsible for Abnormal SERS Enhancement: A DFT Study. *J. Phys. Chem. C* **2009**, *113*, 18212−18222.
(22) Chang, C. M.; Cheng, C.; Wei, C. M. CO Oxidation on Unsupported Au_{55}, Ag_{55}, and $Au_{25}Ag_{30}$ Nanoclusters. *J. Chem. Phys.* **2008**, *128*, 124710.
(23) Shimizu, K.-i.; Sawabe, K.; Satsuma, A. Self-Regenerative Silver Nanocluster Catalyst for CO Oxidation. *ChemCatChem* **2011**, *3*, 1290−1293.
(24) Popolan, D. M.; Bernhardt, T. M. Communication: CO Oxidation by Silver and Gold Cluster Cations: Identification of Different Active Oxygen Species. *J. Chem. Phys.* **2011**, *134*, 091102.
(25) Bernhardt, T. M.; Socaciu-Siebert, L. D.; Hagen, J.; Wöste, L. Size and Composition Dependence in CO Oxidation Reaction on Small Free Gold, Silver, and Binary Silver−Gold Cluster Anions. *Appl. Catal., A* **2005**, *291*, 170−178.
(26) Qu, Z.; Cheng, M.; Huang, W.; Bao, X. Formation of Subsurface Oxygen Species and Its High Activity toward CO Oxidation over Silver Catalysts. *J. Catal.* **2005**, *229*, 446−458.
(27) Christopher, P.; Xin, H.; Linic, S. Visible-Light-Enhanced Catalytic Oxidation Reactions on Plasmonic Silver Nanostructures. *Nat. Chem.* **2011**, *3*, 467−472.
(28) Min, B. K.; Friend, C. M. Heterogeneous Gold-Based Catalysis for Green Chemistry: Low-Temperature CO Oxidation and Propene Oxidation. *Chem. Rev.* **2007**, *107*, 2709−2724.
(29) Qu, Z.; Cheng, M.; Dong, X.; Bao, X. CO Selective Oxidation in H_2-Rich Gas over Ag Nanoparticles—Effect of Oxygen Treatment Temperature on the Activity of Silver Particles Mechanically Mixed with SiO_2. *Catal. Today* **2004**, *93*−*95*, 247−255.
(30) Lamoth, M.; Plodinec, M.; Scharfenberg, L.; Wrabetz, S.; Girgsdies, F.; Jones, T.; Rosowski, F.; Horn, R.; Schlögl, R.; Frei, E. Supported Ag Nanoparticles and Clusters for CO Oxidation: Size Effects and Influence of the Silver−Oxygen Interactions. *ACS Appl. Nano Mater.* **2019**, *2*, 2909−2920.
(31) Dey, S.; Chandra Dhal, G.; Mohan, D.; Prasad, R. Synthesis of Silver Promoted CuMnOx Catalyst for Ambient Temperature Oxidation of Carbon Monoxide. *J. Sci.: Adv. Mater. Devices* **2019**, *4*, 47−56.
(32) Hagen, J.; Socaciu, L. D.; Le Roux, J.; Popolan, D.; Bernhardt, T. M.; Wöste, L.; Mitrić, R.; Noack, H.; Bonačić-Koutecký, V. Cooperative Effects in the Activation of Molecular Oxygen by Anionic Silver Clusters. *J. Am. Chem. Soc.* **2004**, *126*, 3442−3443.
(33) Socaciu, L. D.; Hagen, J.; Le Roux, J.; Popolan, D.; Bernhardt, T. M.; Wöste, L.; Vajda, S. Strongly Cluster Size Dependent Reaction Behavior of CO with O_2 on Free Silver Cluster Anions. *J. Chem. Phys.* **2004**, *120*, 2078−2081.
(34) Luo, Z.; Gamboa, G. U.; Smith, J. C.; Reber, A. C.; Reveles, J. U.; Khanna, S. N.; Castleman, A. W., Jr. Spin Accommodation and Reactivity of Silver Clusters with Oxygen: The Enhanced Stability of Ag_{13}. *J. Am. Chem. Soc.* **2012**, *134*, 18973−18978.
(35) Ma, J.; Cao, X.; Xing, X.; Wang, X.; Parks, J. H. Adsorption of O_2 on Anionic Silver Clusters: Spins and Electron Binding Energies Dominate in the Range up to Nano Sizes. *Phys. Chem. Chem. Phys.* **2016**, *18*, 743−748.
(36) Mahmood, A.; Wang, J.-L. Machine Learning for High Performance Organic Solar Cells: Current Scenario and Future Prospects. *Energy Environ. Sci.* **2021**, *14*, 90−105.
(37) Mahmood, A.; Wang, J.-L. A Time and Resource Efficient Machine Learning Assisted Design of Non-Fullerene Small Molecule Acceptors for P3HT-Based Organic Solar Cells and Green Solvent Selection. *J. Mater. Chem. A* **2021**, *9*, 15684−15695.
(38) Mahmood, A.; Irfan, A.; Wang, J. Developing Efficient Small Molecule Acceptors with Sp2-Hybridized Nitrogen at Different Positions by Density Functional Theory Calculations, Molecular Dynamics Simulations and Machine Learning. *Chem.—Eur. J.* **2022**, *28*, No. e202103712.
(39) Mahmood, A.; Irfan, A.; Wang, J.-L. Machine Learning and Molecular Dynamics Simulations Assisted Evolutionary Design and Discovery Pipeline to Screen the Efficient Small Molecule Acceptors for PTB7-Th Based Organic Solar Cells with over 15% Efficiency. *J. Mater. Chem. A* **2022**, *10*, 4170−4180.
(40) Zaier, R.; Ayachi, S. DFT Molecular Modeling Studies of D-π-A-π-D Type Cyclopentadithiophene-Diketopyrrolopyrrole Based Small Molecules Donor Materials for Organic Photovoltaic Cells. *Optik* **2021**, *239*, 166787.
(41) Irfan, A.; Rasool Chaudhry, A.; Al-Sehemi, A. G. Electron Donating Effect of Amine Groups on Charge Transfer and Photophysical Properties of 1, 3-Diphenyl-1H-Pyrazolo [3, 4-b] Quinolone at Molecular and Solid State Bulk Levels. *Optik* **2020**, *208*, 164009.
(42) Irfan, A.; Al-Sehemi, A. G.; Assiri, M. A.; Ullah, S. Exploration the Effect of Metal and Electron Withdrawing Groups on Charge Transport and Optoelectronic Nature of Schiff Base Ni (II), Cu (II) and Zn (II) Complexes at Molecular and Solid-State Bulk Scales. *Mater. Sci. Semicond. Process.* **2020**, *107*, 104855.
(43) Divya, V. V.; Suresh, C. H. Design and DFT Study of Nitrogen-Rich Donor Systems for Improved Photovoltaic Performance in Dye-Sensitized Solar Cells. *New J. Chem.* **2021**, *45*, 11585−11595.
(44) el-Krim Sandeli, A.; Khiri-Meribout, N.; Benzerka, S.; Boulebd, H.; Gürbüz, N.; Özdemir, N.; Özdemir, İ. Synthesis, Structures, DFT Calculations, and Catalytic Application in the Direct Arylation of Five-Membered Heteroarenes with Aryl Bromides of Novel Palladium-N-Heterocyclic Carbene PEPPSI-Type Complexes. *New J. Chem.* **2021**, *45*, 17878−17892.
(45) Irfan, A.; Chaudhry, A. R.; Al-Sehemi, A. G.; Assiri, M. A.; Hussain, A. Charge Carrier and Optoelectronic Properties of Phenylimidazo [1, 5-a] Pyridine-Containing Small Molecules at Molecular and Solid-State Bulk Scales. *Comput. Mater. Sci.* **2019**, *170*, 109179.
(46) Latosinska, J. N.; Latosinska, M.; Tomczak, M. A.; Medycki, W. Conformational Stability and Thermal Pathways of Relaxation in Triclosan (Antibacterial/Excipient/Contaminant) in Solid-State: Combined Spectroscopic (1H NMR) and Computational (Periodic DFT) Study. *J. Phys. Chem. A* **2015**, *119*, 4864−4874.
(47) Dorotíková, S.; Plevová, K.; Bučinský, L.; Malček, M.; Herich, P.; Kucková, L.; Bobeničová, M.; Šoralová, S.; Kožíšek, J.; Fronc, M.; Milata, V.; Dvoranová, D. Conformational, Spectroscopic, and Molecular Dynamics DFT Study of Precursors for New Potential Antibacterial Fluoroquinolone Drugs. *J. Phys. Chem. A* **2014**, *118*, 9540−9551.
(48) Arulaabaranam, K.; Muthu, S.; Mani, G.; Irfan, A. Conformational Study, FT-IR, FT-Raman, Solvent Effect on UV−Vis, Charge Transfer and Protein−Ligand Interactions of Methyl-2-Pyrazinecarboxylate. *J. Mol. Liq.* **2021**, *341*, 116934.
(49) Klacar, S.; Hellman, A.; Panas, I.; Grönbeck, H. Oxidation of Small Silver Clusters: A Density Functional Theory Study. *J. Phys. Chem. C* **2010**, *114*, 12610−12617.
(50) Wang, C.; Yang, Y.; Liu, X.; Li, Y.; Song, D.; Tian, Y.; Zhang, Z.; Shen, X. Dissociative Chemisorption of O_2 on Ag_n and Ag N− 1 Ir (N= 3−26) Clusters: A First-Principle Study. *Phys. Chem. Chem. Phys.* **2020**, *22*, 9053−9066.

https://doi.org/10.1021/acsomega.2c01437
ACS Omega 2022, 7, 19687−19693

(51) Liao, M.-S.; Watts, J. D.; Huang, M.-J. Theoretical Comparative Study of Oxygen Adsorption on Neutral and Anionic Ag_n and Au_n Clusters (N= 2−25). *J. Phys. Chem. C* **2014**, *118*, 21911−21927.
(52) Frisch, M. J.; Trucks, G. W.; Schlegel, H. B.; Scuseria, G. E.; Robb, M. A.; Cheeseman, J. R.; Scalmani, G.; Barone, V.; Petersson, G. A.; Nakatsuji, H.; Li, X.; Caricato, M.; Marenich, A. V.; Bloino, J.; Janesko, B. G.; Gomperts, R.; Mennucci, B.; Hratchian, H. P.; Ortiz, J. V.; Izmaylov, A. F.; Sonnenberg, J. L.; Williams; Ding, F.; Lipparini, F.; Egidi, F.; Goings, J.; Peng, B.; Petrone, A.; Henderson, T.; Ranasinghe, D.; Zakrzewski, V. G.; Gao, J.; Rega, N.; Zheng, G.; Liang, W.; Hada, M.; Ehara, M.; Toyota, K.; Fukuda, R.; Hasegawa, J.; Ishida, M.; Nakajima, T.; Honda, Y.; Kitao, O.; Nakai, H.; Vreven, T.; Throssell, K.; Montgomery, J. A., Jr.; Peralta, J. E.; Ogliaro, F.; Bearpark, M. J.; Heyd, J. J.; Brothers, E. N.; Kudin, K. N.; Staroverov, V. N.; Keith, T. A.; Kobayashi, R.; Normand, J.; Raghavachari, K.; Rendell, A. P.; Burant, J. C.; Iyengar, S. S.; Tomasi, J.; Cossi, M.; Millam, J. M.; Klene, M.; Adamo, C.; Cammi, R.; Ochterski, J. W.; Martin, R. L.; Morokuma, K.; Farkas, O.; Foresman, J. B.; Fox, D. J. *GaussView 5.0*; Gaussian, Inc.: Wallingford CT, 2016.
(53) Joshi, K.; Krishnamurty, S.; Dar, M. A. Surface Functionalization: An Efficient Alternative for Promoting the Catalytic Activity of Closed Shell Gold Clusters. *Phys. Chem. Chem. Phys.* **2020**, *22*, 23351−23359.
(54) Demichelis, R.; Bruno, M.; Massaro, F. R.; Prencipe, M.; De La Pierre, M.; Nestola, F. First-principle Modelling of Forsterite Surface Properties: Accuracy of Methods and Basis Sets. *J. Comput. Chem.* **2015**, *36*, 1439−1445.
(55) Zhao, Y.; Khetrapal, N. S.; Li, H.; Gao, Y.; Zeng, X. C. Interaction between O_2 and neutral/charged Au_n (n = 1-3) Clusters: A Comparative Study Between Density Functional Theory and Coupled Cluster Calculations. *Chem. Phys. Lett.* **2014**, *592*, 127−131.
(56) Dar, M. A.; Krishnamurty, S. Molecular and Dissociative Adsorption of Oxygen on Au−Pd Bimetallic Clusters: Role of Composition and Spin State of the Cluster. *ACS Omega* **2019**, *4*, 12687−12695.
(57) Chen, M.; Dyer, J. E.; Li, K.; Dixon, D. A. Prediction of Structures and Atomization Energies of Small Silver Clusters,$(Ag)_n$, N< 100. *J. Phys. Chem. A* **2013**, *117*, 8298−8313.
(58) Manzoor, D.; Pal, S. Reactivity and Catalytic Activity of Hydrogen Atom Chemisorbed Silver Clusters. *J. Phys. Chem. A* **2015**, *119*, 6162−6170.
(59) Manzoor, D.; Krishnamurty, S.; Pal, S. Endohedrally Doped Gold Nanocages: Efficient Catalysts for O_2 Activation and CO Oxidation. *Phys. Chem. Chem. Phys.* **2016**, *18*, 7068−7074.
(60) Manzoor, D.; Krishnamurty, S.; Pal, S. Contriving a Catalytically Active Structure from an Inert Conformation: A Density Functional Investigation of Al, Hf, and Ge Doping of Au_{20} Tetrahedral Clusters. *J. Phys. Chem. C* **2016**, *120*, 19636−19641.
(61) Gao, Y.; Shao, N.; Pei, Y.; Chen, Z.; Zeng, X. C. Catalytic Activities of Subnanometer Gold Clusters (Au_{16}−Au_{18}, Au_{20}, and Au_{27}−Au_{35}) for CO Oxidation. *ACS Nano* **2011**, *5*, 7818−7829.
(62) Liu, C.; Tan, Y.; Lin, S.; Li, H.; Wu, X.; Li, L.; Pei, Y.; Zeng, X. C. CO Self-Promoting Oxidation on Nanosized Gold Clusters: Triangular Au_3 Active Site and CO Induced O−O Scission. *J. Am. Chem. Soc.* **2013**, *135*, 2583−2595.

https://doi.org/10.1021/acsomega.2c01437
ACS Omega 2022, 7, 19687−19693